CHAPTER IV

BUBBLES–EXPERIMENTAL

IV.a Experimental Procedure

Several groups have collected experimental data on the two dimensional soap froth. Smith made the first studies using low pressure air in a sealed cell circular glass cell and applied vigorous shaking to produce an initially disordered froth with a few hundred bubbles and a bubble diameter of between one and two millimeters. Coarsening from this length scale to the size of the container required approximately two hours.[206] He photographed the cell periodically during coarsening. With this data Smith measured the rate of area growth with time and Aboav the evolving distribution functions of the froth.[8] Fisher and Fullman preformed a similar experiment in a medium pressure sealed container and independently measured the rate of bubble growth.[86] More recently Weaire and Fu studied the evolution of a froth using very small air bubbles in a cell made from microscope slides and photographed under a microscope.[85] Typical coarsening times for their froth were four or five hours. They were particularly interested in experimentally verifying von Neumann's Law. Glazier, Gross and Stavans collected more complete data on the soap froth in a series of experiments which we describe in detail below.[93,94,220]

Glazier, Gross and Stavans used a series of large rectangular experimental cells. These were made of plexiglass and sized to be slightly smaller than either an $8\frac{1}{2}$" x 11" or $8\frac{1}{2}$" x 14" piece of paper. The vertical spacing was

either 1/8" or 1/16". Catheters inserted through holes drilled in the spacer allowed filling and draining. A thick coat of epoxy sealed the joints.

They used a soap solution consisting, of water (approximately 85% by volume), Dawn brand liquid detergent (approximately 10%) and glycerol (approximately 5%). While they did not attempt to control carefully the mixing of the fluid, their results were apparently independent of the exact fluid composition. However, they found that certain solutions (surprisingly those containing a higher percentage of soap and glycerol) had a higher rate of side breakage than others.

In different runs they used bubbles either of helium or air, helium froths evolving roughly five times faster than air froths, but being otherwise similar. In no case did they observe any evidence of leakage of the working gas from the cell.

Since they were interested only in the long term behavior of the forth, neither Smith nor Fullman made any effort to control the uniformity of their initial bubble pattern. Indeed, the method of froth generation they employed always resulted in highly irregular patterns with broad area and side distributions. Glazier, Gross and Stavans, on the other hand were particularly interested in the transition from ordered to disordered patterns. They therefore developed two basic methods to fill the cell with froth. In the first method, which they used to obtain very uniform fills of small bubbles, they completely filled the cell with soap solution, then tipped the cell on its edge and slowly injected gas bubbles at the bottom of the fluid, draining excess

fluid through a catheter at the bottom of the cell. The variation in the size of the injected bubbles determined the initial degree of disorder in the froth. They found that because of the long fill times (approximately ten minutes), the top portion of the froth was significantly more developed than the bottom at the nominal beginning of the experiment, which made early portions of the time series more difficult to interpret. In the second method, they filled the cell only about 10% full and injected the gas through one of the filling catheters just below the surface of the soap solution. This allowed them to control the size and uniformity of the bubbles both by varying the injection pressure and the angle of the cell relative to the vertical. The advantage of this method was that they could fill the cell more quickly, but it was more difficult to obtain very uniform or very small bubbles.

When necessary they "annealed" the froth by injecting excess fluid and gently tipping the cell to remove obvious irregularities, then draining the excess fluid (their failure to measure the volume of fluid remaining in the cell makes it difficult to provide quantitative estimates of the role of Plateau border broadening), injected a small amount of ink and sealed the catheters with corks and vacuum grease. The ink made the **Plateau borders**, the thickened region of fluid between the membranes and the walls (see Fig. 8), easily visible. To make measurements, they placed the prepared cell level on a photocopier and copied periodically at intervals depending on the rate of evolution (intervals of 15 minutes at early times and 12 or 24 hours at long times). The photocopier has several advantages over photographic recording.

Fig. 8 Plateau Border: Top view of the region where three soap films meet. The films' top surfaces are in contact with a flat glass plate. The wetting of the fluid on the glass sucks excess fluid onto the glass, resulting in the broad lines seen. A similar effect thickens the line where the films meet, which seen from above produces the central triangle. The films themselves are thin, and can be seen to be well centered within the Plateau border (Redrawn from Lewis 1949).[147]

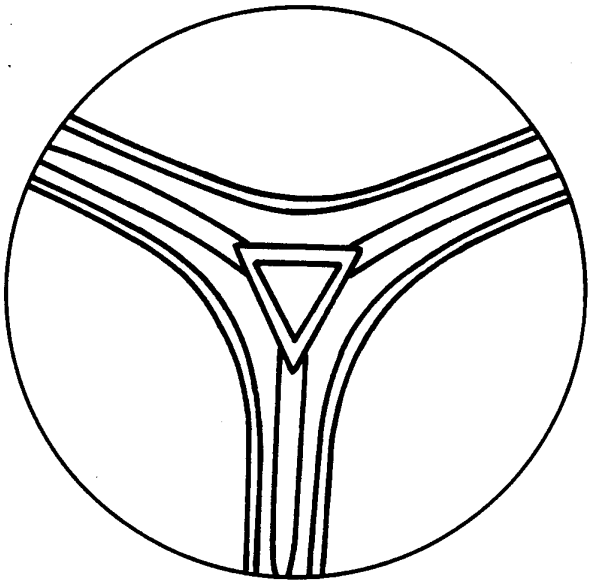

It is simple, much less expensive, and has an intrinsically high contrast ratio. It also produces a large image with correct absolute lengths.

It is important to realize that both photographs and photocopies show the Plateau borders and not the soap membranes themselves. One cannot easily observe the actual position of the soap films nor whether they are curved in the vertical direction. However, examination with a microscope of untinted soap films suggests that the films are both well centered and flat, as seen in Fig. 8.

Glazier, Gross and Stavans used a Xerox model 4000 photocopier which provided relatively low contrast.[94] Stavans and Glazier, and Glazier *et al.* employed a Mita Model DC-1255 photocopier,[93,220] a scanning type which provided much better quality copies, but heated the cell significantly during each copy. While the duration of heating was short, and thus should not have significantly affected the dynamics of the froth, it did result in occasional wall breakage. The total number of walls broken during a run represented less than .1% of the total side redistribution, but nevertheless may have resulted in slightly greater numbers of very many-sided bubble.

IV.b Digitization

Many of the results described for the soap froth were obtained by direct hand counting from photocopies or photographs. Fu, and Glazier Gross and Stavans essentially followed the procedures established by Smith and Aboav, though for area measurements Glazier Gross and Stavans had the

advantage of using a digitizing tablet, a technique also employed by Kreines and Fradkov.[131] Problems with hand digitization include its extreme tedium and large inaccuracies. However, its intrinsic resolution can be very good.

Glazier *et al.* relied on direct digitization of 30% samples of their photocopies using a camera type digitizer with a resolution of 600 x 500 pixels for much of their Potts model and distribution function analysis, editing the digitized images by hand to remove obvious defects in the digitization. Raster images were converted into grains using a standard "worm" technique, each pixel being assigned to a separately numbered grain for analysis. The image quality of their camera digitizer was sufficient that it produced very few spurious bubbles or broken lines (fewer than 2%). The resolution of the digitizer was sufficient to represent a few thousand bubbles with a typical size of 10 x 10 pixels. One advantage of this type of digitization was that the digitized images could serve directly as initial conditions for Potts model simulations, one pixel in the image corresponding to one spin in the model. A disadvantage was that the relatively small image area gave rather poor statistics at long times.

IV.c Basic Experimental Results

IV.c.i Qualitative Description of Coarsening

Let us first look at the qualitative features of the evolution of a soap froth. We distinguish three basic patterns of evolution, that evolving from an initially well ordered state, that evolving from an initially disordered state,

Fig. 9 Evolution of a Soap Froth: Coarsening of a two dimensional soap froth. Illustrations show 15% details of the total area of the experimental cell. (a) The left side shows an initially well ordered run in Helium gas (initial disorder $\partial(0) = 0.17$). Times for the figures: (A) $t = 1$ hour, (B) $t = 2.52$ hours, (C) $t = 4.82$ hours, (D) $t = 8.63$ hours, (E) $t = 19.87$ hours, (F) $t = 52.33$ hours. Letters are keyed to Fig. 16 (d) (b) The right side shows an initially disordered run in air (initial disorder $\partial(0) = 0.85$. Times for the figures: (A') $t = 1.95$ hours, (C') $t = 21.50$ hours, (F') $t = 166.15$ hours. Letters are keyed to Fig. 16 (f). The final states are essentially indistinguishable (From Glazier, Gross and Stavans 1987).[94]

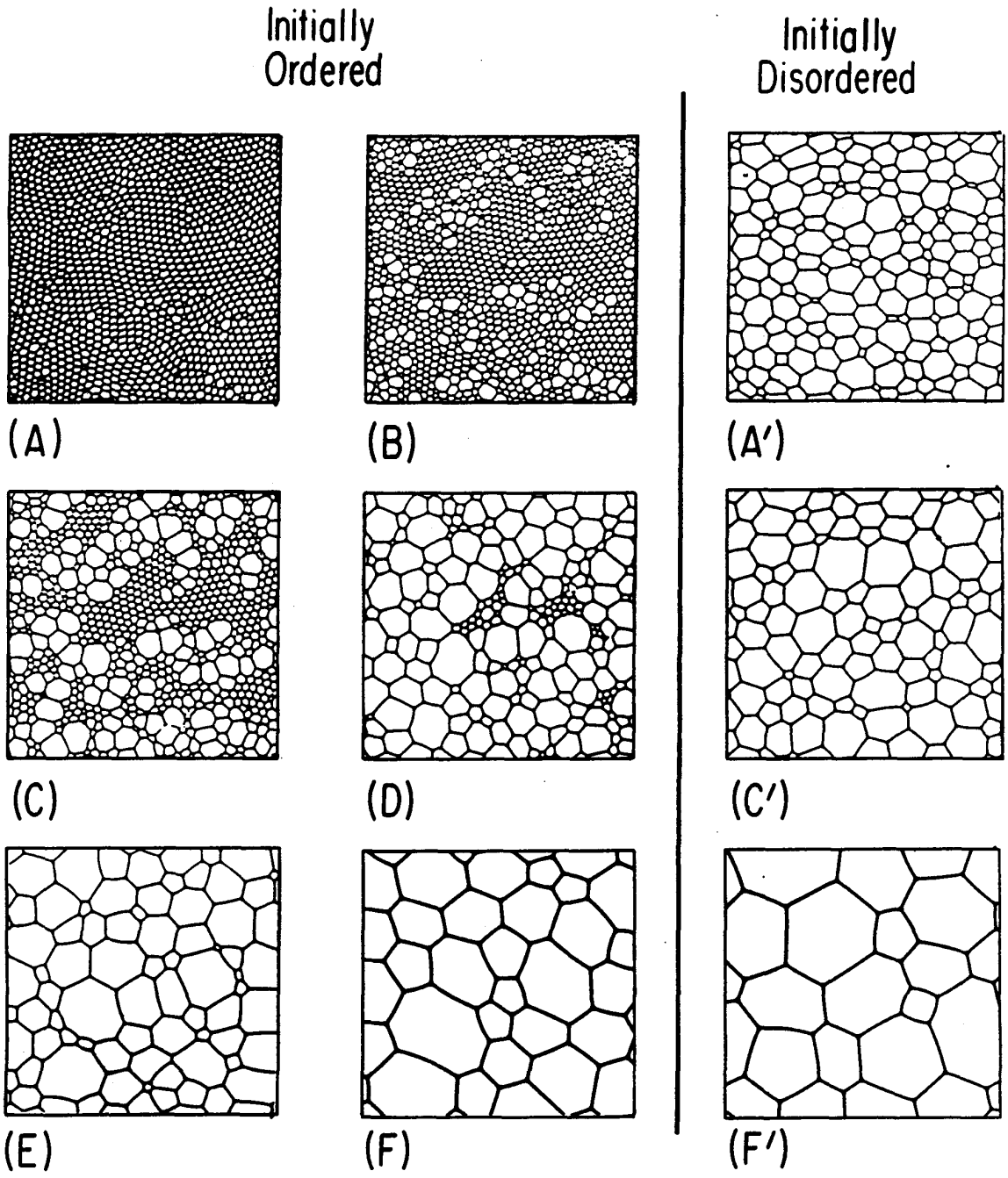
Initially
Ordered
Initially
Disordered
(A)
(B)
(A′)
(C)
(D)
(C′)
(E)
(F)
(F′)
(a)
(b)

Fig. 10 Evolution of a Soap Froth Evolution of an air soap froth with artificially broadened initial distribution functions. Lettered times correspond to regimes in Fig. 16. The illustrated areas represent 5% of the total experimental cell area (From Stavans and Glazier 1989).[220]

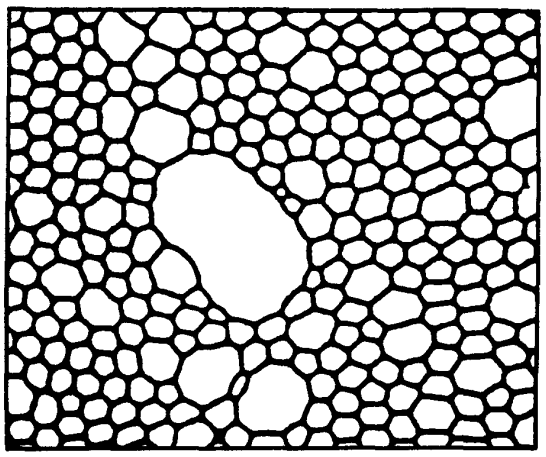

A''

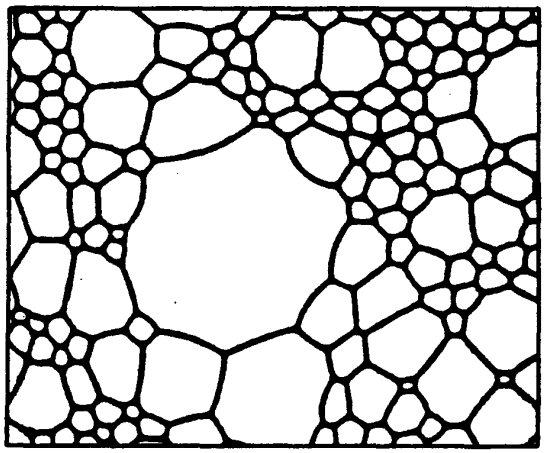

C''

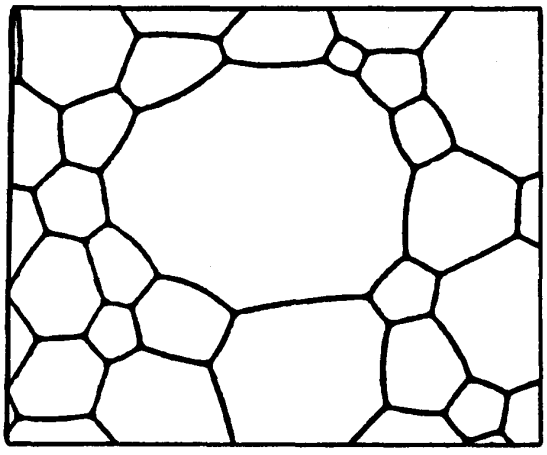

F''

and that evolving from an initial state with an artificially large distribution of initial sizes.

Fig. 9 (a) presents details (corresponding to 15% of total area) of photocopies taken by Glazier, Gross and Stavans of an initially ordered run (with initial disorder to be defined later, $\partial(0) = 0.17$)

We may qualitatively distinguish these figures as follows:

(A) The bubble lattice is essentially ordered, being composed of hexagonal crystal grains with defects consisting of five- and seven-sided bubbles at the grain boundaries. All bubbles are essentially the same size. Most are six-sided. A few are five- or seven-sided. The rate of evolution is slow (See Fig. 16 (d)).

(B) The grain boundaries become visibly marked as five-sided bubbles shrink and seven-sided bubbles grow. However six-sided bubbles do not evolve. The number of bubbles with $n \neq 6$ increases, as does the rate of evolution.

(C) The grain boundaries grow into patches of disorder which eat away at the ordered regions. The ordered and disordered regions occupy essentially equal areas. The normalized width of the area distribution ($\frac{<\delta a>}{<a>}$) is maximal. Many-sided bubbles are common as there is a large probability for a large bubble to be surrounded by much smaller bubbles.

(D) The ordered regions have almost entirely disappeared. The width of the normalized area distribution and the rate of evolution begin to decrease.

The number of many-sided bubbles decreases. The fraction of five-sided bubbles, $\rho(5)$, increases monotonically, while the fraction of six-sided bubbles, $\rho(6)$, decreases. See Fig. 33.

(E), (F) Long term states. The evolution rate is essentially constant. There are almost no three-sided bubbles and many-sided bubbles are rare. However, the fraction of bubbles with more than seven sides, $\rho(n)$, $n > 7$, increases slowly.

For large initial disorder ($\partial_0 = 0.85$), we observe a simpler pattern of evolution. We present detail photos of such a run in Fig. 9 (b).

(A') The lattice is relatively disordered but not in a long term scaling state. The rate of evolution increases monotonically (See Fig. 16 (f)).

(C') The lattice coarsens and the width of the distribution functions first decreases slightly as the system overshoots equilibrium, then increases to its final equilibrium value. The rate of evolution continues to increase monotonically to its final value without overshoot.

(F') Long term state. The state is indistinguishable from (E) and (F).

For an artificially broadened area distribution, including both well ordered and completely disordered patches, we again observe a monotonic equilibration (Fig. 10).

(A") Initial condition. Many small bubbles with a few very large bubbles with very many sides.

(C") The large bubbles gradually lose sides to the advantage of their neighbors. The relative area of many sided bubbles decreases.

(F") Long term states. Except for the presence of one eleven-sided bubble, the state is indistinguishable from (E), (F) and (F').

IV.c.ii von Neumann's Law: Experiment

Fu, Glazier, Gross and Stavans, and Glazier *et al.* have made experimental measurements of von Neumann's law.[85,93,94] Fu measured areas by cutting out the individual bubbles from his photographs and weighing them, an extremely tedious procedure that limited him to small samples. Glazier, Gross and Stavans and Glazier *et al.* made their measurements using a digitizing tablet (marginally less tedious), following around the edge of the bubble and selecting a few key points to digitize. For example a seven-sided bubble might have been digitized as fourteen- or twenty one-sided polygon depending on the degree of curvature of its sides. The digitization was repeated either three or six times for each bubble and the results averaged together to obtain an estimate for the bubble area.

This method had several disadvantages. The most serious problem was the difficulty of making repeated accurate measurements by hand. The typical variation in area estimates for a single bubble could be as high as 5%. Especially for images taken late in a run when the Plateau borders were broad, it was difficult to find the centers of the Plateau borders to obtain the correct perimeter. Enlarging the image increased the error from both

TABLE 3

VON NEUMANN'S LAW

da_n/dt	System				
n	Helium[94] 0.817 (hours)	Helium[94] 11.1 (hours)	Helium[94] 38.23 (hours)	Air[93]	Air[85]
3	–	–	–	-6.94	–
4	–	-1.21	-1.28	-5.28	-0.41
5	-0.59	-0.50	-0.70	-3.04	-0.41
6	0.00	0.00	0.00	0.06	0.005
7	0.71	0.67	0.47	1.39	0.38
8	0.89	1.28	1.04	4.13	0.74
9	–	–	1.82	5.25	1.13
10	–	–	–	8.42	1.29
11	–	–	–	24.47	1.88
12	–	–	–	18.97	–
14	–	–	–	31.18	–
15	–	–	–	19.93	–
17	–	–	–	28.78	–
21	–	–	–	25.13	–
22	–	–	–	47.59	–
24	–	–	–	37.52	–
25	–	–	–	35.00	–
36	–	–	–	23.01	–
66	–	–	–	46.54	–

Fig. 11 Von Neumann's Law. Growth rates for n-sided helium bubbles at (A) $t = 1.82$ hours, (B) $t = 12.10$ hours and (C) $t = 39.23$ hours, for the run given in Fig. 16 (d). Results are consistent with von Neumann's law with $\kappa = 4.57 \text{ x } 10^{-2} \pm 3.8 \text{ x } 10^{-3}$ $\frac{\text{mm}^2}{\text{min}}$ at all times. Error bars indicate the variation in κ among individual n-sided bubbles at 95% certainty (From Glazier, Gross and Stavans 1987).[94]

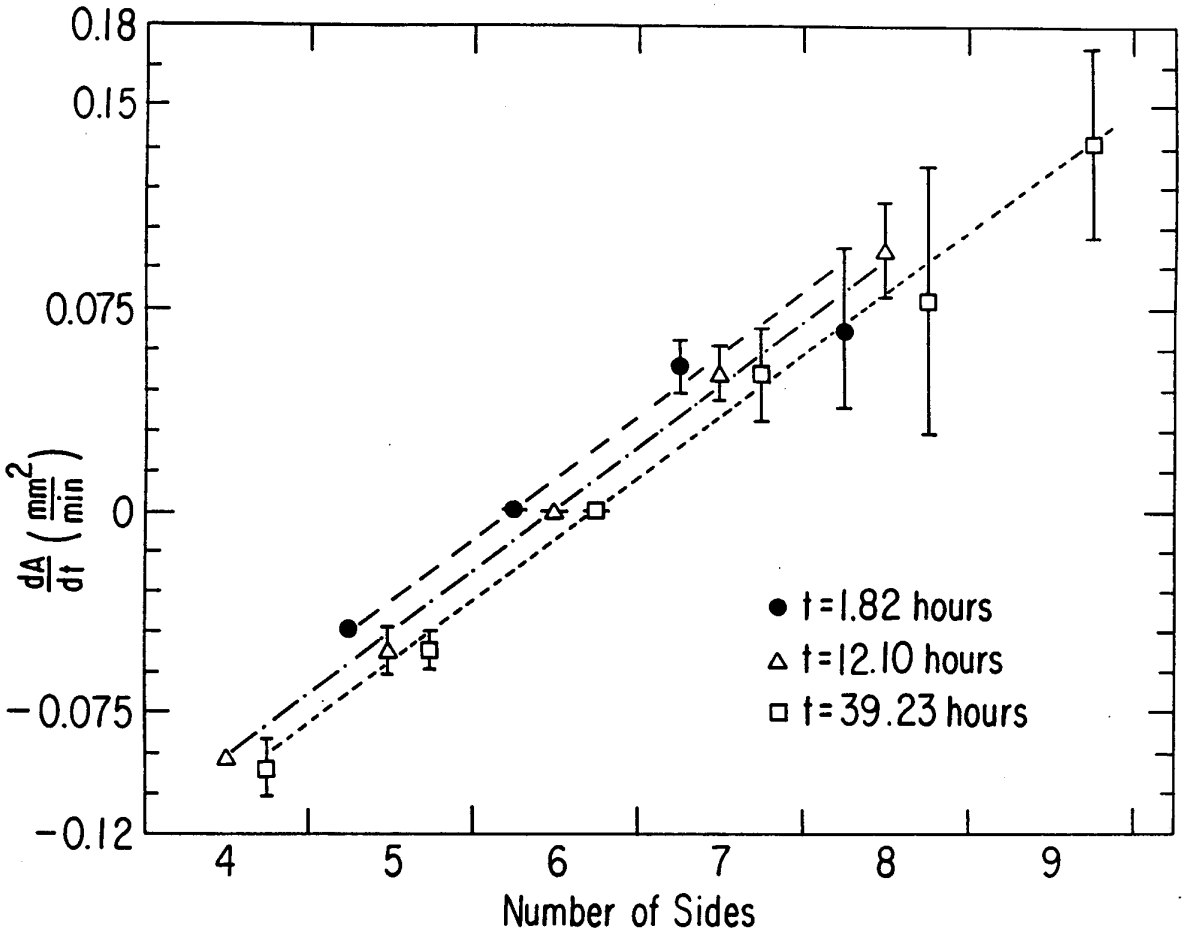
0.18
0.15
0.075
0
−0.075
−0.12
4
5
6
7
8
9
Number of Sides
$\frac{dA}{dt}\left(\frac{mm^2}{min}\right)$
● t=1.82 hours
△ t=12.10 hours
□ t=39.23 hours

Fig. 12 Von Neumann's Law. Growth rates for n-sided air bubbles. The result is consistent with von Neumann's law for n up to 24. Error bars show one standard deviation. Single points indicate that only one measurement was made for that number of sides (From Glazier *et al.* 1989).[93]

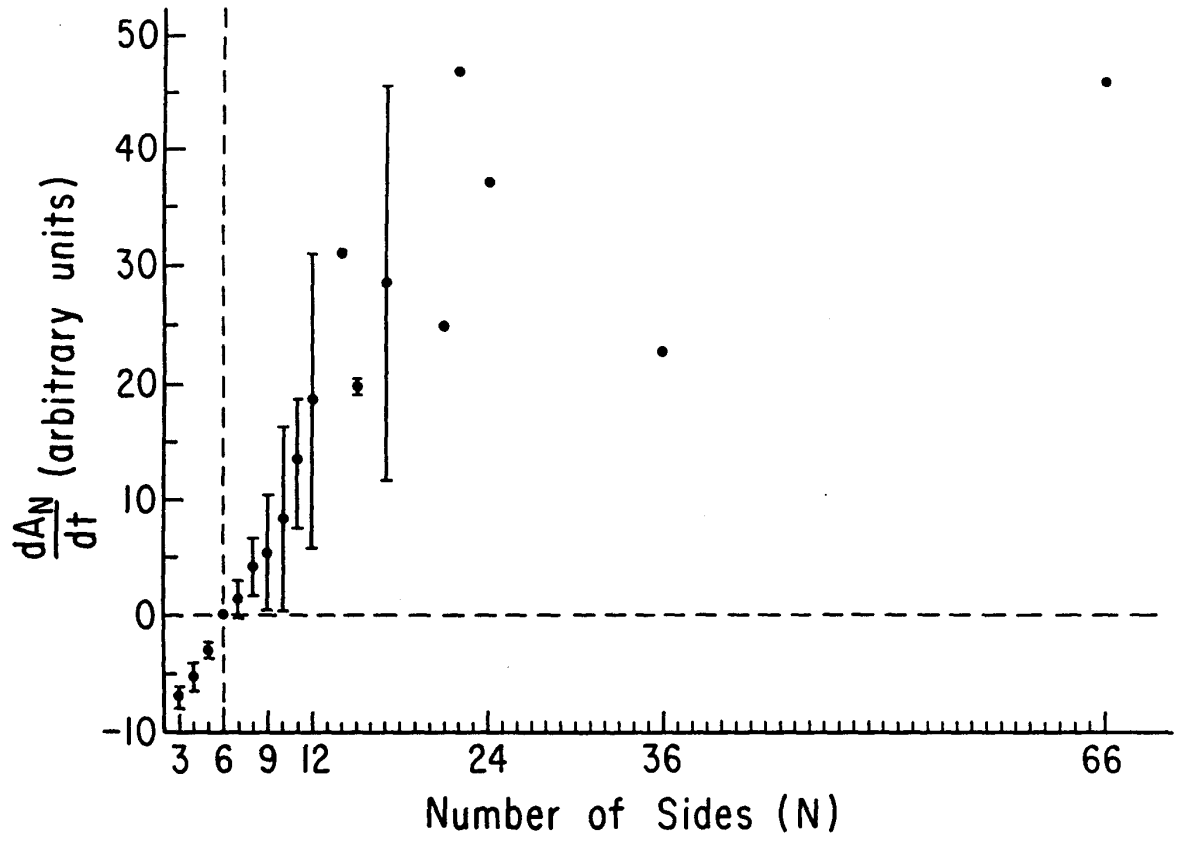
50
40
30
20
10
0
-10
$\frac{dA_N}{dt}$ (arbitrary units)
3 6 9 12 24 36 66
Number of Sides (N)

effects, and working with larger bubbles made the problem worse, since von Neumann's law predicts absolute not relative changes in area. Finally, the measured area depended on the number of points used in the approximating polygon and the exact position where they were set down, thus systematically underestimating the size of bubbles with fewer than six sides and overestimating the size of bubbles with more than six sides.

Measurements made over the longest possible time intervals, i.e. measuring the area of a bubble just after (and again just before) it changed its number of sides, minimize these errors. Large statistical samples reduce the random noise introduced by hand measurement. In the case of bubbles with three or more than ten sides, however, the rarity of the types limited Glazier *et al.*'s sample size to at most a few (sometimes only one) bubbles. Measurements of six-sided bubbles were easier because of the tendency of such bubbles to clump together at early times during a run. Treating a clump of six-sided bubbles as one many-sided bubble greatly reduced the measurement error. The essentially straight walls of six-sided bubbles further improved accuracy in this case.

In Table 3 and Figs. 11 and 12 we present experimental measurements of von Neumann's law by Fu, Glazier, Gross and Stavans, and Glazier *et al.*. Fig. 11 shows a series of measurements made by Glazier, Gross and Stavans in helium at different times during the same experimental run, and shows that the area diffusion constant κ (the slope of the line through each set of points) remained constant to within 5% during the period of the measure-

ments. 12 shows Glazier *et al.*'s results taken at a single time from an air system in which a large range of bubbles sizes and hence number of sides were purposely introduced, providing information on the growth rates of bubbles with up to twenty sides, although not in a scaling state nor with any great statistical accuracy. The indicated error bars in the measured values of $\frac{dA_n}{dt}$ at least partially represent real fluctuations in bubble growth rates. For example, some seven-sided bubbles do shrink. However, much of the scatter is probably due to measurement error rather than intrinsic fluctuations in growth rates. The calculated value of κ depends on the details like the cell thickness and the amount of fluid in the froth, so we neglect it. What is important is the linearity of the measured growth rates in n and the constancy of the diffusion constant in time for a given run.

All three groups obtained the expected linear relation between n and $\frac{dA_n}{dt}$ for bubbles with between five and roughly fifteen sides. Three- and four-sided bubbles shrink slightly more slowly than expected and bubbles with more than about fifteen sides perhaps grow slightly more slowly than expected. The deviation for few-sided bubbles may be due to the stabilizing effect of the Plateau borders on very small bubbles. It may also be due to the deviations observed in the internal angles of few-sided bubbles discussed below. The slow growth rate of many-sided bubbles may be due partially to angle deviations but since this cannot result in a saturation, merely a reduction in the slope of the n dependence, its origin is not completely explained.

Since it is not possible to produce an experimental cell large enough to

generate a twenty-sided bubble in a scaling state, Glazier *et al.* made the observations quoted above for many-sided bubbles using froths with artificially introduced many-sided bubbles.

Experimentally Stavans and Glazier observed (Fig. 10) that many-sided bubbles tend to lose sides continuously in time.[220] Mathematically, we may start from equation III.15:

$$\frac{dN}{dt} = -\sum_{n=3,4,5} \frac{\kappa\rho(n)N(n-6)}{\lambda_n < a >}, \tag{III.15}$$

the number of bubbles lost per unit time. If the total area of the experimental cell is A, then $< a >= A/N$ so

$$\frac{d < a >}{dt} = \sum_{n=3,4,5} \frac{\kappa\rho(n)(n-6)}{\lambda_n}, \tag{IV.1}$$

i.e.,

$$< a(t) >= t \cdot \left(\sum_{n=3,4,5} \frac{\kappa\rho(n)(n-6)}{\lambda_n} \right) + a_0, \tag{9}$$

where a_0 is the average area at the start of the experiment. Substituting approximate experimental values for $\rho(n)$ and λ_n, we find

$$< a >= a_0 + 0.8\kappa t. \tag{IV.3}$$

On the other hand, an n-sided bubble will have area

$$A_n = A_n(0) + (n-6)\kappa t \tag{IV.4}$$

The ratio is

$$\lim_{t\to\infty} \frac{A_n(0) + (n-6)\kappa t}{a_0 + 0.8\kappa t} = 1.25 \cdot (n-6). \tag{IV.5}$$

Fig. 13 Internal Angles in the Soap Froth. Average internal angles versus n for n-sided bubbles. Note that angles are smaller than 120° for few-sided bubbles and larger for many-sided bubbles so that bubbles are more polygonal than expected. Error bars show one standard deviation of the measurement. Ten bubbles were measured for small n, fewer for large n (From Stavans and Glazier 1989).[220]

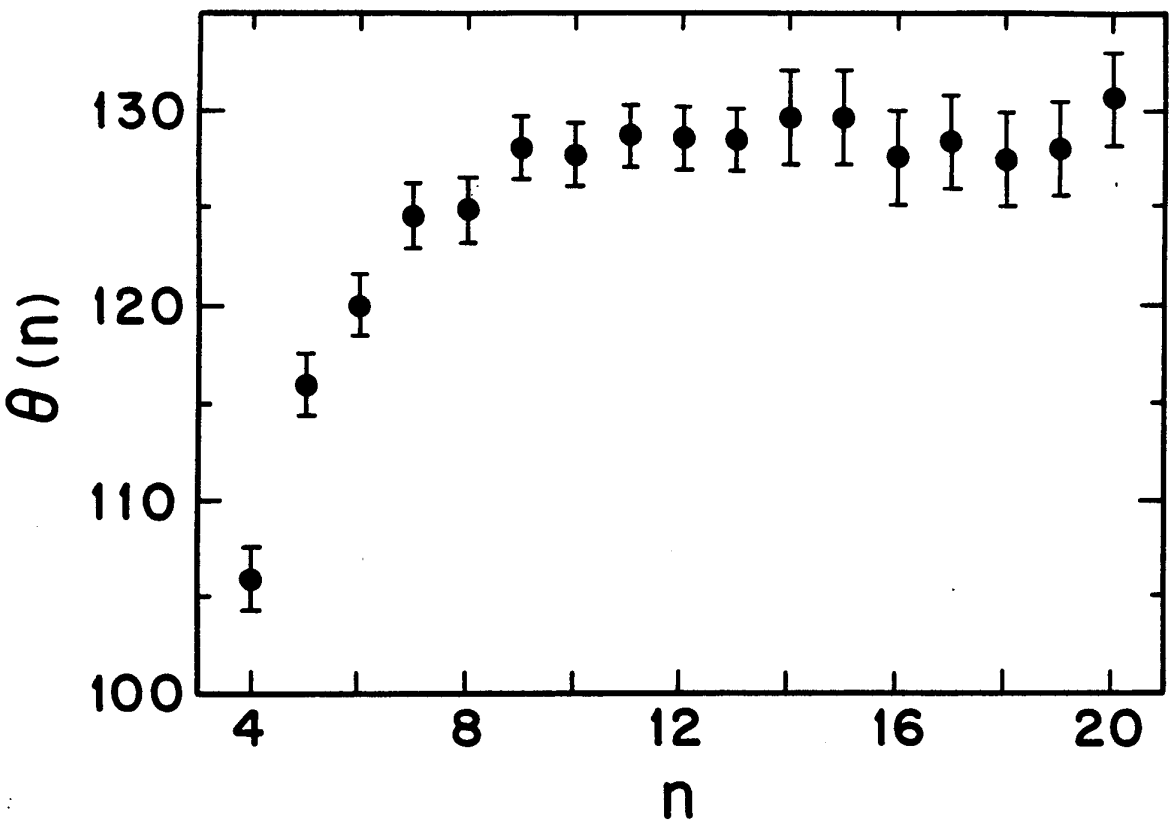
130
120
110
100
θ(n)
4
8
12
16
20
n

Fig. 14 Modified Von Neumann's Law. Growth rates for n-sided bubbles predicted by von Neumann's Law using the measured angle deviations in Fig. 13 (boxes) and ideal von Neumann's Law (solid line). The large error in the measured value of $\theta(3)$, means that we cannot tell if small bubbles shrink slower than a liner law would predict.

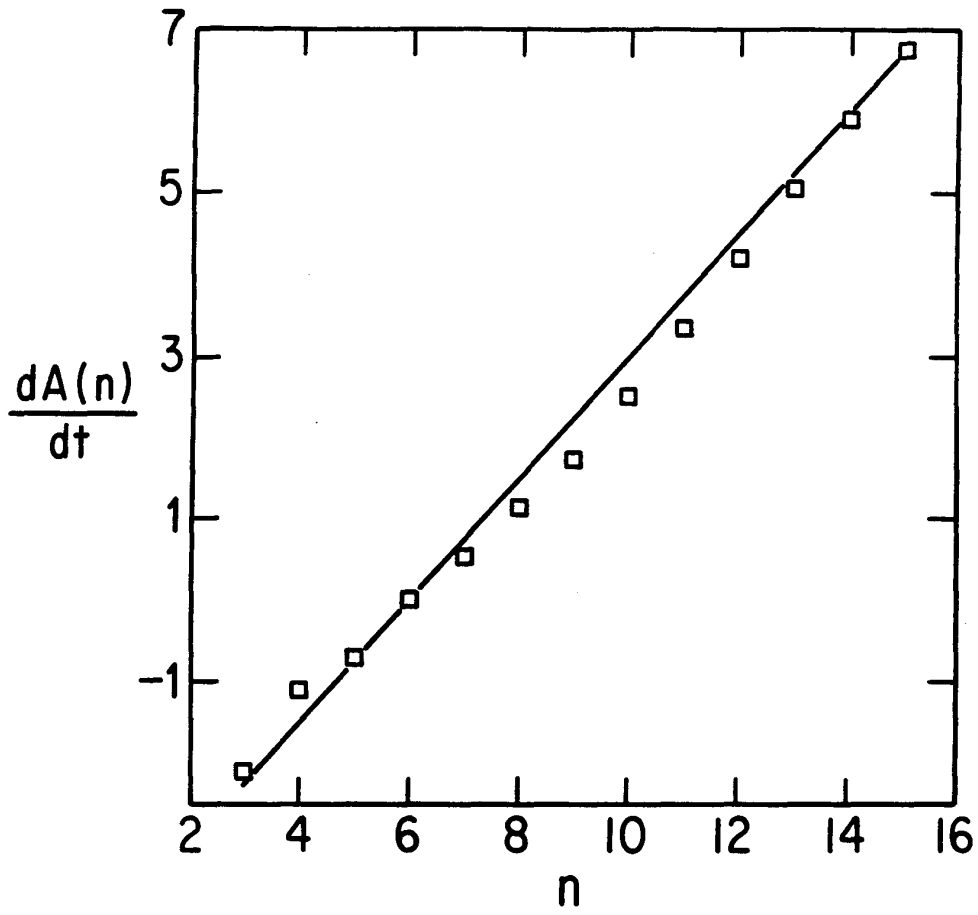
7
5
3
1
-1
dA(n)
dt
2
4
6
8
10
12
14
16
n

Fig. 15 Area Growth in Soap Froths. (A) Average area versus time in a low pressure two dimensional air froth (From Smith 1952).[206] (B) Number of bubbles (equivalent to normalized average area) versus time in a medium pressure two dimensional air froth. Circles are experimental data, x's Fullman's vertex model (From Fullman 1952).[86]

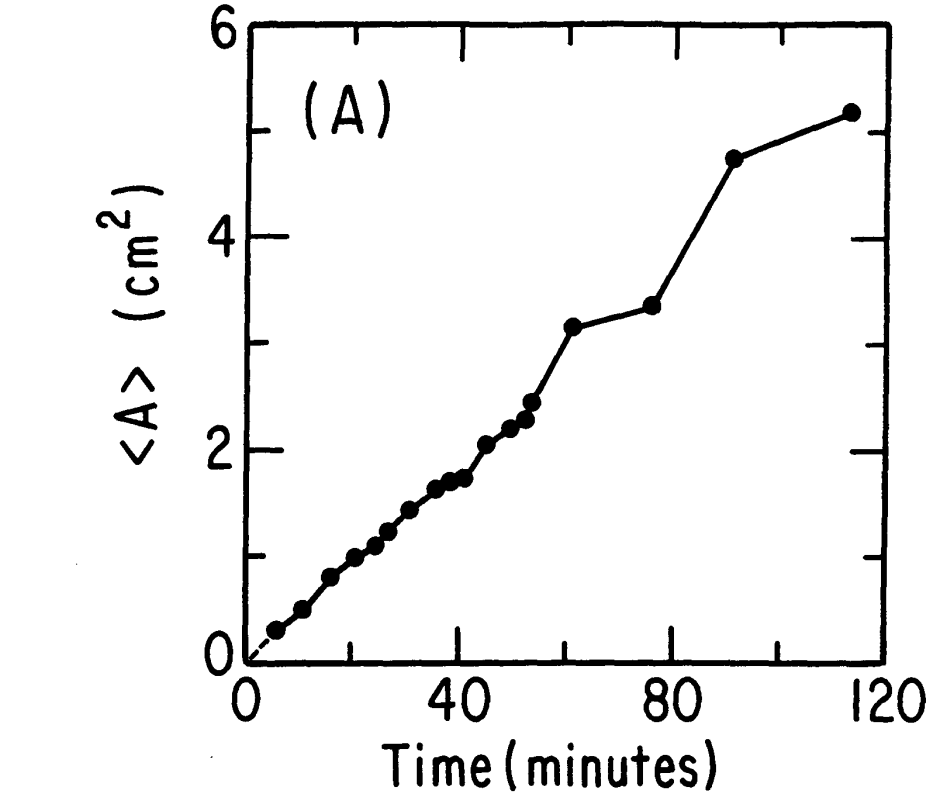
(A)
<A> (cm²)
6
4
2
0
0
40
80
120
Time (minutes)

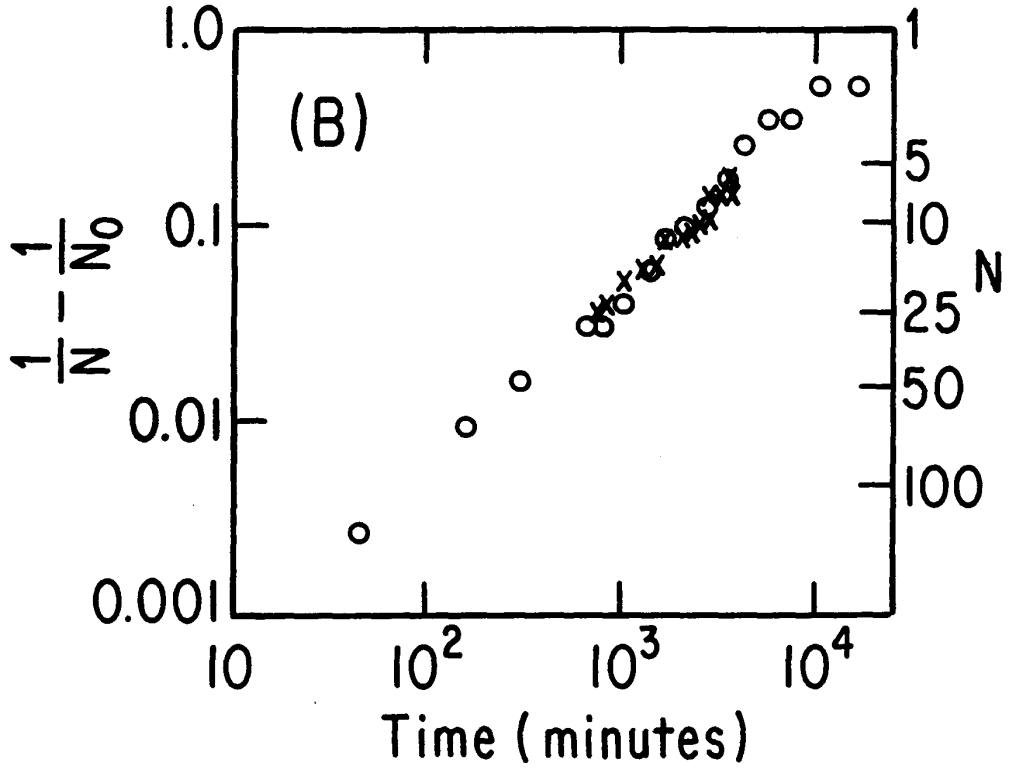
(B)
1 − 1/N
1 − 1/N₀
1.0
0.1
0.01
0.001
10
10²
10³
10⁴
Time (minutes)
1
5
10
25
50
100
N

Fig. 16 Area Growth in Soap Froths. Disorder parameter and number of bubbles in a fixed area cell (equivalent to average area) versus time for increasingly disordered initial conditions, (a) $\partial(0) = 0.04 \pm 0.02$, $\alpha = 0.63 \pm 0.03$ (Helium 1/16" cell thickness), (b) $\partial(0) = 0.08 \pm 0.01$, $\alpha = 0.50 \pm 0.01$ (Helium 1/8" cell thickness), (c) $\partial(0) = 0.11 \pm 0.02$, $\alpha = 0.50 \pm 0.04$ (Air 1/8" cell thickness), (d) $\partial(0) = 0.17 \pm 0.04$, $\alpha = 0.68 \pm 0.03$ (Helium 1/8" cell thickness), (e) $\partial(0) = 0.33 \pm 0.01$, $\alpha = 0.53 \pm 0.01$ (Helium 1/16" cell thickness), (f) $\partial(0) = 0.85 \pm 0.05$, $\alpha = 0.81 \pm 0.08$ (Air 1/8" cell thickness). Errors are at 90% certainty. Capital letters in (d) and (f) indicate times referred to in the text and in Fig. 9. Dots are experimental values. Solid lines and values of α are best fits computed from the phenomenological model of Glazier, Gross and Stavans.[94] Dashed lines are the disorder, ∂, as calculated from the model. Initial times are offset to 1 hour. For initially ordered conditions the rate of evolution overshoots its long term value, while for initially disordered conditions, the rate increases monotonically. In both cases the long term states obey a power law, $N \propto t^{-\alpha}$, where, $\alpha = 0.59 \pm 0.11$ (From Glazier, Gross and Stavans 1987).[94]

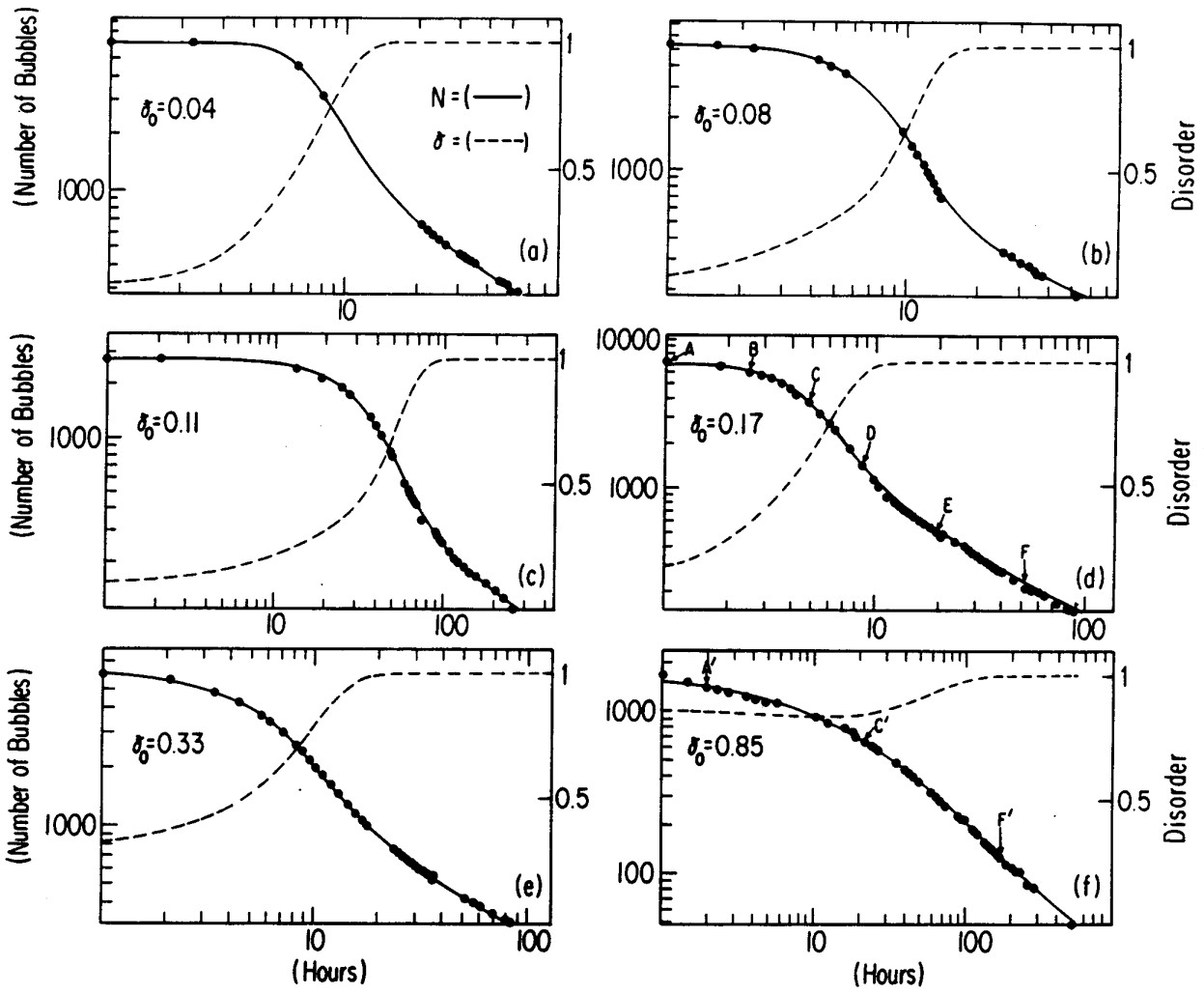
(Number of Bubbles)
Disorder
N = (——)
δ = (----)
δ0=0.04
δ0=0.08
δ0=0.11
δ0=0.17
δ0=0.33
δ0=0.85
(a)
(b)
(c)
(d)
(e)
(f)
A
B
C
D
E
F
A'
C'
F'
1000
10000
100
10
0.5
1
(Hours)

Fig. 17 Area Growth in Soap Froths. Average area (in pixels) versus time for a two dimensional air froth in a large cell. Dots are experimental data. Circles are values from a Potts model simulation starting from identical initial conditions (From Glazier *et al.* 1989).[93]

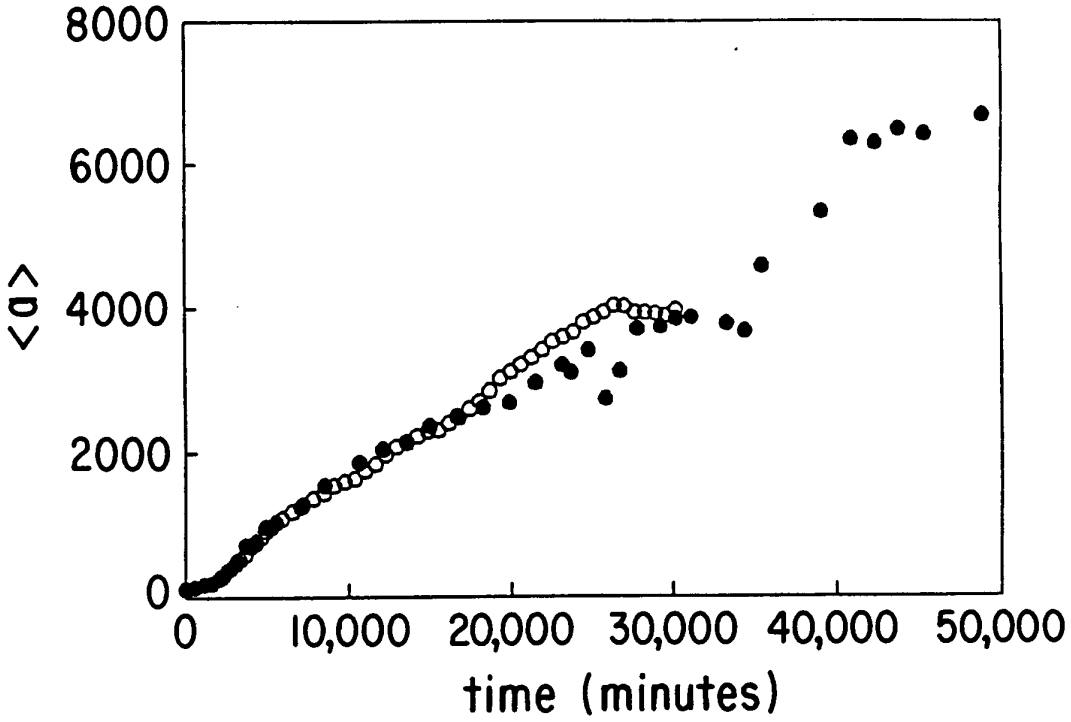
8000
6000
4000
2000
0
<D>
0
10,000
20,000
30,000
40,000
50,000
time (minutes)

Thus many-sided bubbles should equilibrate slowly, on a timescale of order $\frac{A_n(0)}{(n-6)\kappa}$. In the absence of side shedding this relation would predict that the average relative areas of n-sided bubbles would be proportional to $(n-6)$ which is non-sensical. The equilibration will happen much faster if the rate of side shedding is large. Unfortunately, no one has ever measured the mean rate of side shedding to check these hypotheses. Thompson and Frost have given an alternative argument for the equilibration of a froth.[229]

Stavans and Glazier also measured the average internal angle of an n-sided bubble, $\theta(n)$ by enlarging each vertex, bisecting the Plateau borders near the vertex, and measuring the internal angles with a protractor. Once again, their chief source of error was finding the true position of the centers of the Plateau borders.

In Fig. 13 we present their measurements of the average internal angles for the same run shown in the von Neumann's law calculation in Fig. 13. They found small but significant deviations from the expected 120° angles. In particular, the average wall curvature of all bubbles was smaller in magnitude, i.e. bubbles were more polygonal, than expected. In Fig. 14 we show the modified von Neumann's law obtained from these values of $\theta(n)$ and the linear predictions of the ordinary von Neumann's Law. Within the experimental error we cannot distinguish the two results, though the modified law predicts a smaller absolute rate of growth than the unmodified. The apparent rate of shrinkage of few-sided bubbles is smaller than predicted by a pure linear fit, as observed by Glazier *et al.*

IV.c.iii Quantitative Kinetics

We can begin to make our qualitative ideas about disordering and grain growth more precise by measuring the average area per bubble as a function of time, $< a >$ or $< \mathbf{A} >$. Such measurements have been made in two distinct ways. Fullman, and Glazier Gross and Stavans hand counted the number of bubbles in the experimental cell which were not in contact with the cell walls and used the total area of the interior of the froth to obtain the average bubble size.[86,94] Smith, Aboav, and Glazier *et al.* measured bubble areas directly, either by weighing cut outs from photographs or by digitizing the images.[8,93,206]

We present results for average bubble area versus time in Fig. 15 (A) (Smith's results), Fig. 15 (B) (Fullman's results), Fig. 16 (Glazier, Gross and Stavan's results, converted back into the number of bubbles needed to cover the experimental cell completely), and Fig. 17. (Glazier *et al.*'s results obtained by direct digitization of a 30% sample of an air run). The letters in Fig. 16 (d) and (f) key to the regimes of evolution presented in Fig. 9. In Fig. 17 the slight non-monotonicity results from the fact that large bubbles are more likely to touch the frame boundary and hence to be excluded from the ensemble.

These quantitative measurements confirm division of the evolution into distinct regimes. For an initially ordered froth we observe a period of slow growth, followed by a period of equilibration during which the average area per bubble increases roughly exponentially, and finally a scaling regime dur-

TABLE 4

GROWTH EXPONENTS

Experiment		Two Dim.	Three Dim.
Group	System	α	α
Soap Froths			
Smith[206]	Froth	1	–
Fischer[86]		1	–
Aboav[8]		2	–
Glasier and Stavans[94]		0.59 ±0.11	–
Glasier *et al.*[93]		1	–
Lipid Monolayers Metal Grains			
Moore *et al.*[169]	stearic acid	1.10 ± 0.10	–
	Lead		
Bolling and Winegard[32]	Pb 10^{-6} Pure	–	0.8 ± 0.05
	Pb + 0.005% Ag	–	0.96
	Pb + 0.01% Ag	–	0.96
	Pb + 0.02% Ag	–	1.04
	Pb + 0.04% Ag	–	1.14
	Pb + 0.005% Au	–	1.12
	Pb + 0.02% Au	–	1.20
Drolet and Galbois[59]	Ultra Pure	–	0.82
	Tin		
Holmes and Winegard[107]	10^{-5} Pure	–	1.00 ± 0.02
Drolet and Galbois[259]	Ultra Pure	–	0.86
	Aluminum		
Gordon[260]	Ultra Pure	–	0.5
Beck *et al.*[261]	High Purity		
	400° C	–	0.18
	600° C	–	0.64
	Al + 2% Mg		
	400° C	–	0.34
	600° C	–	0.90
	Al + .6% Mg		
	550° C	–	0.3
	650° C	–	0.68
Beck[24]	Pure		
	350° C	–	0.112
	600° C	–	0.644
	"Near Melting"	–	1
Fradkov *et al.*[262]	Al $+10^{-4}$ Mg Foil	1	–

TABLE 4, *continued*

Experiment		Two Dim.	Three Dim.
Group	System	α	α
Metal Grains			
	α-Brass		
Beck and Burke[259]	70:30	–	0.4
Beck[24]	Ultra Pure	–	1
	Commercial	–	0.4
Fullman[86]	450° C	–	0.42
	850° C	–	0.6
Beck[24]	High Purity		0.8
Burke[260]	500° C	–	0.7
	850° C	–	1
Fullman[86]	500° C	–	0.70
	850° C	–	1.2
	Iron		
Miller[261]	Carbon Steel		
	815° C	–	0.16
	1250° C	–	0.44
Hu[262]	Ultra Pure Fe	–	0.80
Ceramics			
Dutta and Sprigs[263]	ZnO	–	0.66
Kapadia and Liepold[264]	MgO	–	1
Gordon *et al.*[265]		–	0.66
Petrovic and Ristic[266]	CdO	–	0.66
Tien and Subbaro[267]	$Ca_{.16}Zr_{.84}O_{1.84}$	–	0.8
Kingery and François[268]	UO_2	–	0.66

TABLE 4, *continued*

Theory		Two Dim.	Three Dim.
Group	System	α	α
	Mean Field Theories		
Burke and Turnbull[42]	Radius Based	1	1
Hillert[106]		1	1
Feltham[259]		1	1
Mullins[172,173]		1	1
Rhines and Craig[260]		–	1
Louat[152]		1	–
Novikov[183]		0.91	–
Hunderi and Ryum[112]		1	–
Hunderi and Ryum[114]		0.77 ± 0.3	–
Mullins[173]	Topological	1	–
Marder[157]		1	–
	Boundary Models		
Frost *et al.*[52]		1	–
	Vertex Models		
Fullman[86]		1	–
Enamoto *et al.*[261]		1	–
Weaire and Kermode[242,243]		2	–
	Network Models		
Fradkov *et al.*[76]		1	–
Beenakker[27,26]		1	–
	Potts Models		
Anderson *et al.*[16]		0.83	–
Wejchert *et al.*[249]	Initial Voronoi	0.84 ± 0.06	–
	Initial Hard Sphere	0.98 ± 0.06	–
Anderson *et al.*[14]	Q=36	0.87	–
	Q=48	0.90	–
	Q=64	0.94	–
Anderson *et al.*[13,15]		0.98 ± 0.04	0.96 ± 0.12

ing which $< a >$ increases as a power law. For an initially disordered froth we find a monotonic increase in growth rate until it reaches the equilibrium power law. We have not measured growth rates for an artificially broadened initial distribution, but we expect that the growth rate will decrease monotonically to its equilibrium value, as observed in simulations of Frost and Thompson.[83] Smith and Fullman both begin with disordered states and obtain $< a > \sim t$ at all times.[86,206]

While finite size effects may well be important in the latter stages of pattern evolution, the range of rollover points from equilibrating to scaling behavior observed (ranging from 1000 bubbles for Fig. 16 (a) and (d) to 100 bubbles in Fig. 16 (c)) suggests that the transition between these two regimes is not an edge effect. To further control for edge effects Glazier, Gross and Stavans counted the number of bubbles touching the lateral walls of the cell (edge bubbles) as a function of time. If the average area of a bubble in contact with the edge were a constant times the average area of a bubble in the bulk, we would expect $N_{edge} \propto N_{bulk}^{0.5}$. This would be the case if the edge behaved as a non-interacting window on an infinite cell or as an infinite network of hexagonal bubbles. In either case the result would suggest that edge effects were insignificant. They found $N_{edge} \propto N_{bulk}^{0.56 \pm 0.14}$ which was consistent with either hypothesis.

In the scaling state the coarsening of the froth may be described by a scaling exponent, α, $< a(t) > \propto t^{\alpha}$. Smith and Fullman both measured $\alpha = 1$ but with relatively few bubbles. Aboav, reanalyzing Smith's data found $\alpha = 2$.[8]

Glazier, Gross and Stavans obtained a value of $\alpha = 0.59(^{+0.11}_{-0.09})$, where the scaling exponent was determined using an indirect method discussed below. Finally, Glazier *et al.*, working in a larger experimental cell, obtained results consistent with, though not conclusively demonstrating, $\alpha = 1$. Observations of coarsening in thin film and bulk metals, alloys and ceramics have yielded a similar variety of exponents, though non-von Neumann factors like impurity pinning and three dimensional effects complicate the interpretation. In general we find that higher impurity concentrations lead to lower growth exponents as impurities zone refine to grain boundaries and act as pinning centers which eventually reduce boundary mobilities to zero. Some impurities (e.g. Au in Pb), however, apparently enhance grain boundary mobility or grain coalescence, and thus increase the growth exponent. Higher temperatures nearly always result in higher growth exponents since they reduce grain freezing due to anisotropy and other pinning effects. In two dimensions, preferential etching or oxidation at grain boundaries can also reduce boundary mobilities and growth exponents. Measured exponents in bulk and thin films, metals, alloys and ceramics are all comparable. We summarize a few selected experimental measurements and theoretical predictions of the scaling exponent in Table 4. Where the original result was presented for the average radius rather than the average area, the quoted value of α is twice the radius exponent. This approximation is correct in the case of a scaling state. Three dimensional results are given for two dimensional sections of three dimensional volumes.

Summarizing: most experimental coarsening has $0.3 < \alpha < 1$ and the majority of models give $\alpha = 1$. We observe experimental results close to the theoretical values for α, only when the experiment is carefully controlled, a large experimental cell and many bubbles in the soap froth, high temperatures and pure materials in grain growth. At short times and for initially well ordered conditions the transient during which a soap froth equilibrates results in a larger apparent exponent measured by Glazier, Gross and Stavans, hence Aboav's measurement of a growth exponent of two (we will discuss later the reasons we believe that Aboav measured an equilibrating rather than a scaling state). At very long times in the froth, we suspect that the effective diffusion constant of the soap films decreases due to broadening of the Plateau borders, hence the smaller apparent exponent. In grain growth we have mentioned a variety of effects that can lead to smaller long term exponents and even the complete cessation of coarsening. The most important of these mechanisms are impurity segregation due to local zone refining resulting in pinning of grain boundaries (an effect which can be observed in a correctly designed soap froth experiment) and pinning of grain boundaries due to strong orientational anisotropies in surface energies (which can be duplicated in Potts model simulations).

The essential unanimity of the theoretical predictions of the growth exponent, and the experimental uncertainties in measuring it,

TABLE 5

PLATEAU BORDER BROADENING

Run 1		Run 2	
Time (hours)	Width(mm)	Time (hours)	Width(mm)
0.00	0.393 ± 0.028	0.00	0.309 ± 0.019
11.08	0.430 ± 0.027	2.50	0.313 ± 0.018
56.43	0.475 ± 0.019	18.47	0.312 ± 0.024
139.08	0.512 ± 0.028	42.75	0.313 ± 0.024
490.45	0.590 ± 0.034	74.20	0.394 ± 0.037
–	–	258.08	0.602 ± 0.031

Fig. 18 Plateau Border Broadening. Plateau border widths versus time for two air runs. Run 1 (circles). Run 2 (squares).

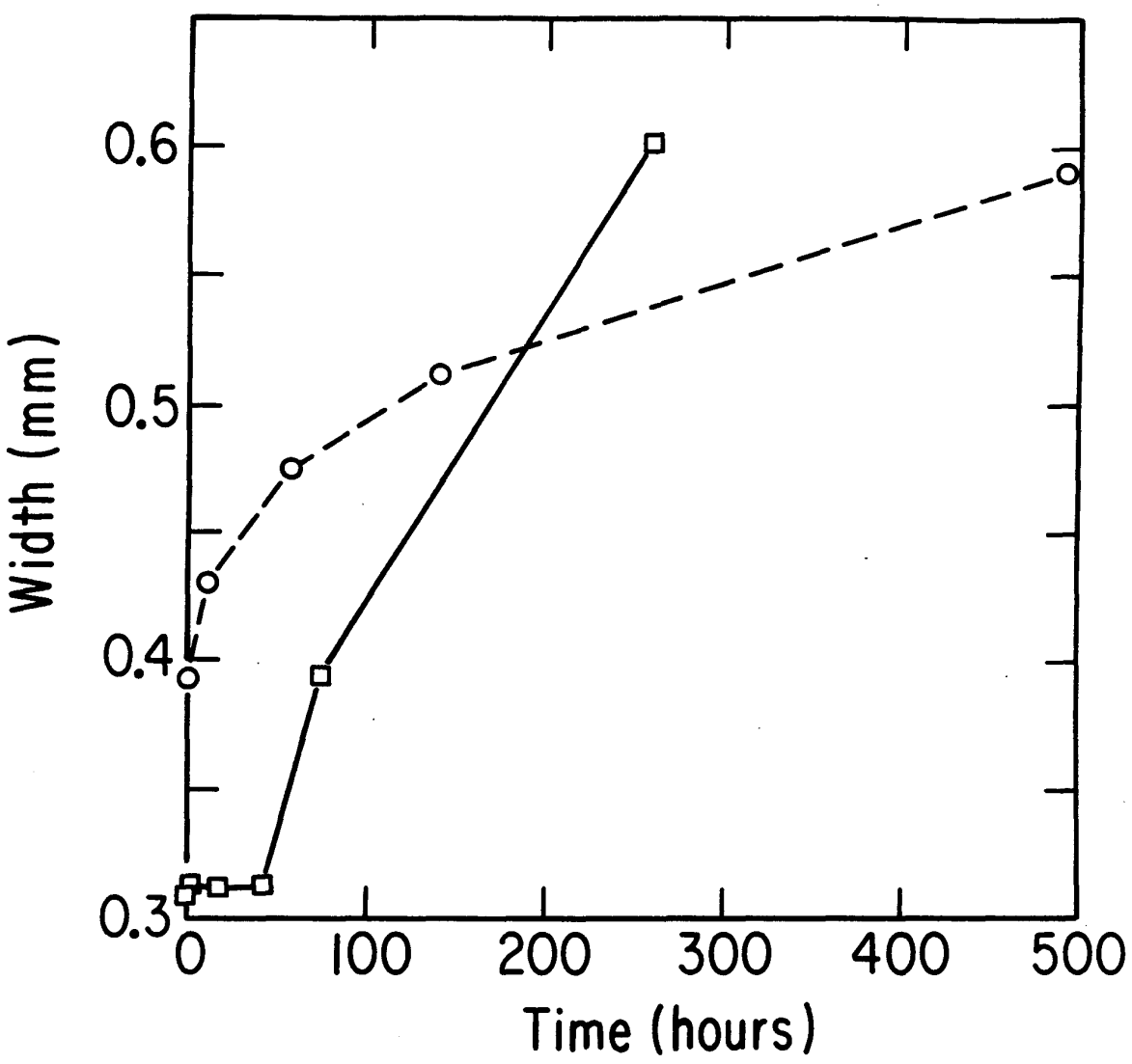
0.6
0.5
0.4
0.3
Width (mm)
0
100
200
300
400
500
Time (hours)

suggest that a better test of the agreement between theory and experiment is the theory's ability to duplicate the observed transient behaviors for initially ordered and initially disordered patterns.

IV.d Other Topics

IV.d.i Broadening of Plateau Borders

Glazier, Gross and Stavans originally proposed that the anomalous exponent they observed in the two dimensional soap froth resulted from the failure of the froth to reach a scaling state.[94] Later work has demonstrated that their froths did reach a well behaved scaling state.[93,220] Others have suggested that boundary effects play a role when many bubbles are in contact with the walls of the experimental cell.[157,200] However, the experiments of Smith, and Fullman showed no such anomalous exponent though they worked with even fewer bubbles.[86,206] The Potts model simulations of Glazier *et al.* did show a boundary effect glitch in the long time tail of the simulation (See Fig. 17), just where the experiment showed a sudden decrease in growth rate, but this similarity may be fortuitous.[93] One possible source of the difference is that Glazier, Gross and Stavans used a rectangular cell, while Smith and Fullman used a round cell. A later experiment by Glazier *et al.* in a larger cell where edge effects should have been less important was consistent with an exponent of $\alpha = 1$.

The observation of anomalously low growth exponents is common in metals, where initially well dispersed impurities gradually segregate to the grain

boundaries and reduce boundary mobility and hence slow (or even stop) grain growth. Inversely, the presence of impurities which increase boundary mobility can result in growth exponents larger than 1.[24] In a froth the equivalent to a decreased boundary mobility is a decreased diffusion constant of the soap films. While changes in the chemical structure of the films as they age are possible, it seems more likely that any decrease in diffusion constant is due to the increase of the amount of fluid per unit length of soap film in the sealed cell, as bubbles disappear and the total length of the soap film decreases. Film thickening *per se* is probably not too important since the thickness of the soap films depends on the competition between van der Waals attractive forces and electrical double layer forces between the lipid monolayers on the surface of the film,[176] and since the Plateau borders take up most of the excess fluid.[220] However, even a small amount of film thickening would result in a large decrease in diffusion constant.

An additional experimental problem is that we have no techniques to measure the film thickness directly during a coarsening run. The Plateau border width can be measured directly. Since we might expect that the film thickness would increase with the widths of the Plateau borders which indicate the amount of excess fluid present in the froth, a measurement of Plateau border broadening cannot hope to separate the two effects definitively. Of course, if we could measure the von Neumann κ accurately as a function of time we could check the constancy of the diffusion constant directly, and correct our models without recourse to physical explanations.

Against the diffusion constant explanation lies Glazier, Gross and Stavans' measurement of the constancy of the von Neumann κ discussed in the previous section. The helium run in question, however, gave a growth exponent of $\alpha = 0.68$ and would have given a still larger exponent (nearly 1) if the data had been cut at the time of the last diffusion constant measurement. There is thus no real evidence for the constancy of κ in the tail of the time evolution where the anomalous growth rates occurred.

Determining the fraction of the soap film obstructed by the Plateau borders was not straightforward. Glazier could measure only the widths of the borders, not their vertical extent, and even measuring the widths from the experimental photocopies proved unreliable, because the changes in width during the experiment were comparable to the uncertainties in the widths in the copies. In particular, the photocopier proved to be anisotropic in its treatment of lines. Some orientations produced smooth well defined lines, and some irregular lines with great variations in line width. Examination of an actual froth with a magnifying glass showed that this was indeed an artifact of the photocopies and not an exotic wetting effect of the plexiglass. He therefore measured only lines oriented within 30° of the axis giving the smoothest line profiles. We present the results for two air runs in an $\frac{1}{8}$" cell in Table 5 and Fig. 18. In the first run the width of the Plateau borders doubled during the run, in the second the increase was approximately 50%.

If we assume that the vertical extent of a Plateau border is roughly one half its horizontal extent we obtain the following results (A larger wetting

angle would result in a relatively larger obstructed area and hence in an effect of greater magnitude). In the first run the fraction of the film obstructed by the Plateau Borders ranged from approximately 12.4% at the beginning of the run to 18.7% at the end. The growth exponent for this run was $\alpha = 0.81$. In the second run the obstructed fraction grew from 9.9% at the beginning of the run to 19.0% at the end. The growth exponent for this run was $\alpha = 0.50$. The Plateau border width in the second run did not increase significantly until the number of bubbles decreased to fewer than two hundred. The fact that a lower exponent corresponds to a larger percentage increase in obstructed area is suggestive but hardly conclusive. Even more suggestive was the exponent of nearly one obtained by Glazier *et al.* in a much larger cell which showed little Plateau border broadening. Also favoring Plateau border broadening is the difference in average exponent between cells with a height of 1/8" ($\alpha = 0.71$) and 1/16" ($\alpha = 0.58$). We would expect that Plateau border broadening, but not film thickening, would have a larger effect in a thinner cell.

To obtain a definitive measure of the growth exponent in the soap froth, we need to repeat the grain growth measurement in a drained cell where the width of the Plateau borders, and hence the film thickness, is held constant.

IV.d.ii Disappearance of Four- and Five-Sided Bubbles

Many of the models we will discuss require the enumeration of the different fundamental processes by which a bubble can change its number of sides. In particular, they depend on the rate of side swapping ($T1$ processes) and

the rate at which three-, four- and five-sided bubbles disappear. Smith, in his original article, claimed that only three-sided bubbles could disappear directly, and that four- and five-sided bubbles always shed sides as they shrank to become three-sided when they were very small.[206] Glazier, Gross and Stavans, on the other hand, claimed that 50% of four-sided bubbles and 10% of five-sided bubbles disappeared directly.[94] Later Stavans and Glazier revised their estimate for the rate of direct disappearance by five-sided bubbles to 24%.[220] Fu also observed direct disappearance, though he did not publish estimates for the relevant rates.[85] A theoretical study by Weaire supports the contention that arbitrarily small four- and five-sided bubbles may be stable against side shedding.[237] However, the distinction may be more a matter of definition than a true physical difference. Very small bubbles are sensitive to the thickness of the cell and are hence no longer two dimensional in their properties. In particular, when a cylindrical bubble disappears, it first pinches off on the bottom plate (where the Plateau borders are broader due to gravity) to form a conical bubble, and then shrinks rapidly before disappearing on the top plate. Since Smith took his photographs from the top, he recorded the disappearance of the conical bubble, while Glazier *et al.* photocopying from below, recorded the initial separation. Since the conical bubbles behave in a manner qualitatively different from the ensemble of cylindrical bubbles, the latter definition seems more sensible.